

The Dynamics of Affleck-Dine Condensate Collapse

KARI ENQVIST¹

Department of Physics and Helsinki Institute of Physics,

P.O. Box 9, FIN-00014 University of Helsinki, Finland

AND

JOHN McDONALD²

Department of Physics and Astronomy, University of Glasgow, Glasgow G12 8QQ, Scotland

August 25, 2018

Abstract

In the MSSM, cosmological scalar field condensates formed along flat directions of the scalar potential (Affleck-Dine condensates) are typically unstable with respect to formation of Q-balls, a type of non-topological soliton. We consider the dynamical evolution of the Affleck-Dine condensate in the MSSM. We discuss the creation and linear growth, in F- and D-term inflation models, of the quantum seed perturbations which in the non-linear regime catalyse the collapse of the condensate to non-topological soliton lumps. We study numerically the evolution of the collapsing condensate lumps and show that the solitons initially formed are not in general Q-balls, but Q-axitons, a pseudo-breather which can have very different properties from Q-balls of the same charge. We calculate the energy and charge radiated from a spherically symmetric condensate lump as it evolves into a Q-axiton. We also discuss the implications for baryogenesis and dark matter.

¹enqvist@pcu.helsinki.fi; ²mcdonald@physics.gla.ac.uk

1 Introduction

Affleck-Dine (AD) baryogenesis [1] is a natural candidate for the origin of the baryon asymmetry [2] in the context of the MSSM and its extensions [3], with potentially important consequences for cosmology such as observable isocurvature perturbations [4], non-thermal relic neutralinos [5] and number densities of baryons and dark matter particles which are similar [6, 7]. The original picture of AD baryogenesis was of a homogeneous squark condensate formed along an F- and D-flat direction of the MSSM scalar potential, in which an asymmetry is induced via non-renormalizable soft SUSY-breaking terms. This subsequently thermalizes or decays, leaving the observed baryon asymmetry. More recently it was shown that the homogeneous AD condensate is typically unstable with respect to spatial perturbations [6, 8]. This is because the potential along flat directions of the MSSM scalar potential usually deviates from a pure ϕ^2 potential, resulting in a negative pressure whenever the potential is flatter than ϕ^2 . Such deviations can occur because of A-terms in the potential [9], because of a sharp change in the scalar mass term at large field values (gauge-mediated SUSY breaking models [8, 10]), or because of radiative corrections from the gauge sector (conventional gravity-mediated SUSY breaking models [6, 7]). It is the latter on which we will focus here. Although the main interest in unstable scalar field condensates along MSSM flat directions is perhaps AD baryogenesis, we emphasize that the phenomenon can arise for any coherently oscillating scalar field along a flat direction of the MSSM scalar potential with gauge interactions. This is because the gauge corrections will cause the mass squared term of the flat direction to decrease with increasing scale [6]. In the present view of post-inflationary SUSY cosmology, the formation of such coherently oscillating scalar field condensates is a common and natural occurrence, as a result of order H corrections to the SUSY breaking terms in the scalar potential [11, 12]. In the following we will generically refer to the complex scalar field as the Affleck-Dine (AD) scalar.

Spatial "seed" perturbations in the AD condensate, arising from quantum fluctuations of the AD scalar during inflation, will grow and eventually go non-linear, forming

condensate lumps [6, 7]. However, up until now there has been no clear picture of what happens to the lumps once they go non-linear. It has been assumed that they eventually reach their lowest energy state for a given global charge, namely a Q-ball [13]. One aim of the present paper is to clarify the non-linear evolution of these condensate lumps. We will see that the condensate lumps generally do not initially form Q-balls, but rather a higher energy state which we refer to as a Q-axiton. These are somewhat similar to the original axitons [14] (a form of pseudo-breather soliton [15]) which form in the case of a real axion field, but in our case they can carry a charge by virtue of the complex nature of the AD scalar. Only in the case where the original AD condensate is carrying a near maximal charge are the properties of the Q-axitons close to those of Q-balls of a similar charge.

For some of the important applications of Q-balls to cosmology, the ratio of the charge trapped in baryonic Q-balls (B-balls) to the total charge, f_B , plays an important role [5, 7, 16]. A second goal of this paper is to estimate f_B for various examples.

The paper is organized as follows. In section 2 we discuss the cosmology of flat directions in SUSY models. In section 3 we discuss the quantum seed fluctuations. In section 4 we discuss the linear evolution of the spatial perturbations of the AD field. In section 5 we study numerically the non-linear evolution of a spherically symmetric condensate lump and estimate f_B for various examples. In section 6 we discuss the implications for AD baryogenesis and late-decaying Q-ball cosmology. In section 7 we summarize our conclusions.

2 MSSM Flat Directions in Cosmology

An F- and D-flat direction of the MSSM with gravity-mediated SUSY breaking has a scalar potential of the form [6, 7]

$$U(\Phi) \approx (m^2 - cH^2) \left(1 + K \log \left(\frac{|\Phi|^2}{M^2} \right) \right) |\Phi|^2 + \frac{\lambda^2 |\Phi|^{2(d-1)}}{M_*^{2(d-3)}} + \left(\frac{A_\lambda \lambda \Phi^d}{dM_*^{d-3}} + h.c. \right), \quad (1)$$

where m is the conventional gravity-mediated soft SUSY breaking scalar mass term ($m \approx 100$ GeV), d is the dimension of the non-renormalizable term in the superpotential which lifts the flat direction, cH^2 gives the order H^2 correction to the scalar mass

(with c positive and typically of the order of one for AD scalars [12]) and we assume that the natural scale of the non-renormalizable terms is M_* , where $M_* = M_{Pl}/8\pi$ is the supergravity mass scale [3]. The A-term also receives order H corrections, $A_\lambda = A_{\lambda o} + a_\lambda H$, where $A_{\lambda o}$ is the gravity-mediated soft SUSY breaking term and a_λ depends on the nature of the inflation model; for F-term inflation $|a_\lambda|$ is typically of the order of one [12] whilst for minimal D-term inflation models it is zero [17].

The logarithmic correction to the scalar mass term, which occurs along flat directions with Yukawa and gauge interactions, is crucial for the growth of perturbations of the AD field and the formation of Q-balls [6, 7]. This growth occurs if $K < 0$, which is usually the case for AD scalars with gauge interactions, since K is dominated by gaugino corrections [6]. For flat directions with squark fields, $K \approx -(0.1 - 0.01)$ [6, 7]. The actual value depends on the nature of the flat direction; in practice we will mostly be concerned with the case of baryonic Q-balls made of squarks.

If cH^2 is positive at the end of inflation, the AD scalar will be at a non-zero minimum of its potential. Once $H \lesssim m$, the AD scalar will begin to coherently oscillate around its minimum at zero and the A-term will induce a global charge asymmetry in the condensate [1, 12, 16]. The resulting asymmetry in the Universe at present is then proportional to the reheating temperature after inflation (T_R),

$$\eta_B = \frac{2\pi n_B T_R}{H^2 M_{Pl}^2}, \quad (2)$$

where η_B is the present baryon to entropy ratio and n_B and H are the baryon charge density and the expansion rate when the asymmetry is formed ($H \approx m$) [7]. We see that, because of the dependence on T_R , the baryon asymmetry in AD baryogenesis cannot be determined independently of the inflation model; in practice, we can use the present baryon asymmetry to *fix* the reheating temperature and so determine the background cosmology. In general, the Universe will be matter dominated by coherently oscillating inflatons when the B asymmetry forms at $H \approx m$, since the thermal gravitino upper bound on T_R , $T_R \lesssim 10^9$ GeV [18], implies that the value of H when the inflaton matter domination period ends at T_R is less than 1 GeV.

3 Seed Perturbations

3.1 Growth of Perturbations

Just like for the inflaton, there will be a spectrum of spatial perturbations induced in the AD scalar field by quantum fluctuations during inflation [6]. For fields of mass $m \lesssim H$, the scalar fields have fluctuations on leaving the horizon of magnitude

$$\delta\phi \approx \frac{H}{2\pi} . \quad (3)$$

In general, the equations of motion for perturbations about the minimum of the potential have the form,

$$\delta\ddot{\phi} + 3H\delta\dot{\phi} - \nabla^2\delta\phi = -kH^2\delta\phi , \quad (4)$$

where k is determined by the parameters c , $|a_\lambda|$ and d of the AD potential. For perturbations larger than the horizon, the spatial derivative can be ignored, since the perturbation can be treated as homogeneous on sub-horizon scales. During inflation (with $H = H_I = \text{constant}$), the solution of Eq.(4) for the amplitude of larger than horizon perturbations is

$$\delta\phi \propto a^{-Re(\sigma)} \quad ; \quad \sigma = \frac{1}{2} \left[3 - \sqrt{9 - 4k} \right] . \quad (5)$$

$k > 9/4$ gives a damped and oscillating solution for $\delta\phi$, for which the suppression of the amplitude of the perturbation by the expansion of the Universe is maximal, whilst $k < 9/4$ gives a purely damped solution. In general, $Re(\sigma) \leq 3/2$. During the matter dominated period following inflation (with $H \propto a^{-3/2}$), the solution for the amplitude of $\delta\phi$ is

$$\delta\phi \propto a^{-Re(\eta)} \quad ; \quad \eta = \frac{1}{2} \left[\frac{3}{2} - \sqrt{\frac{9}{4} - 4k} \right] . \quad (6)$$

$k > 9/16$ gives a damped and oscillating solution for $\delta\phi$, with maximal amplitude suppression, whilst $k < 9/16$ gives a purely damped solution. In general, $Re(\eta) \leq 3/4$. Thus when the perturbation re-enters the horizon during matter domination, the amplitude is given by

$$\delta\phi_{hor} = \left(\frac{a_e}{a_{hor}} \right)^{Re(\eta)} \frac{e^{-Re(\sigma)\Delta N_e(\lambda)} H_I}{2\pi} , \quad (7)$$

where $\Delta N_e(\lambda)$ is the number of e-foldings before the end of inflation at which a perturbation of scale λ exits the horizon, a_e is the scale factor at the end of inflation and a_{hor} is the scale factor when the perturbation re-enters the horizon. Once inside the horizon, the spatial derivatives become important. For $\frac{k^2}{a^2} \gtrsim H^2$ and $H \gtrsim m$, the spatial derivative dominates the potential term and $\delta\phi \propto a^{-1}$. Thus, writing in terms of the scale λ at H during matter domination, the perturbation spectrum once the perturbation is within the horizon is given by

$$\delta\phi(\lambda) \approx \frac{(H^2 H_I \lambda^3)^x}{2\pi\lambda}; \quad x = 1 - \frac{2}{3}Re(\eta) - \frac{1}{3}Re(\sigma). \quad (8)$$

For the case with the largest suppression of the amplitude ($k > 9/4$), $Re(\sigma) = 2Re(\eta) = 3/2$, so that $x = 0$ and the resulting spectrum is very simple¹

$$\delta\phi(\lambda) \approx \frac{1}{2\pi\lambda}. \quad (9)$$

An important feature of the spectrum in what follows is that the perturbation is usually larger for smaller values of λ .

3.2 Perturbations of the Affleck-Dine Field

The actual value of k is determined by the form of the AD scalar potential. Let $\Phi = (\phi_1 + i\phi_2)/\sqrt{2}$ and let k_1 and k_2 be the values of k for $\delta\phi_1$ and $\delta\phi_2$. In general, choosing the phase of Φ such that λA_λ is real and negative, the minimum of the potential is at $\phi_2 = 0$ and $\phi_1 = \phi_{1m}$, with

$$\phi_{1m} = \left(\frac{c}{\alpha}\right)^{\frac{1}{2(d-2)}} H^{\frac{1}{d-2}}; \quad \alpha = \frac{\lambda^2(d-1)}{2^{d-2} M_*^{2(d-3)}}, \quad (10)$$

where for simplicity we are considering the A-term along the ϕ_1 direction to be negligible when minimizing; in general it results in a correction of order one to the ϕ_1 minimum. During inflation, H is constant and, on perturbing about the $(\phi_{1m}, 0)$ minimum, we obtain equations of the form of Eq.(4) with

$$k_1 = c(2d-4) \quad (11)$$

¹This differs from the spectrum given in [6], which assumed a constant mass term throughout for the perturbation.

for $\delta\phi_1$ and

$$k_2 = |a_\lambda| (d-1)^{1/2} c^{1/2} \quad (12)$$

for $\delta\phi_2$.

During the matter dominated period the minimum of the AD potential is time-dependent. As a result, when we perturb about $\phi_{1\,m}$ by $\Delta\phi_1$, we obtain

$$\Delta\ddot{\phi}_1 + 3H\Delta\dot{\phi}_1 = \frac{9}{4} \frac{(d-3)}{(d-2)^2} H^2 \phi_{1\,m} - c(2d-4)H^2 \Delta\phi_1 . \quad (13)$$

Thus ϕ_1 will not oscillate about $\phi_{1\,m}$, but rather about a larger value given by

$$\phi_1(t) = \left(1 + \frac{9(d-3)}{8c(d-2)^3}\right) \phi_{1\,m} . \quad (14)$$

Perturbing (ϕ_1, ϕ_2) about the $(\phi_1(t), 0)$ effective minimum then gives equations of the form of Eq.(4) with

$$k_1 = c(2d-4) + \frac{9}{4} \frac{(d-3)(2d-3)}{(d-2)^2} \quad (15)$$

and

$$k_2 = \frac{9}{4} \frac{(d-3)}{(d-2)^2} + |a_\lambda| (d-1)^{1/2} c^{1/2} \left(1 + \frac{9(d-3)}{8c(d-2)^2}\right) . \quad (16)$$

If $a_\lambda = 0$, as in D-term inflation models, then the solution for the evolution of $\delta\phi_2$ is simply $\delta\phi_2 \propto \phi_1(t)$. This is easily understood, as in this limit there is no potential along the θ direction of the AD field and so $\delta\theta = \delta\phi_2/\phi_1$ is constant.

From this we see that, in general, the evolution of the ϕ_1 and ϕ_2 perturbations at $H \gtrsim m$ can be different, depending on c , d and a_λ . However, for c and $|a_\lambda| \approx 1$, as expected in F-term inflation models, it is likely that $k_i > 9/4$ and so the amplitude of $\delta\phi_1$ and $\delta\phi_2$ will be equally (i.e. maximally) suppressed throughout. In this case $\delta\phi_1 \approx \delta\phi_2$ at $H \approx m$. We will focus on this case in the following. For $|a_\lambda| = 0$, as expected in D-term inflation models, $\delta\phi_2 \propto \phi_1$ and so $\delta\theta$ is constant. In this case $\delta\phi_2$ can be much larger than $\delta\phi_1$ at $H \approx m$.

To discuss the evolution of the perturbations at $H \lesssim m$, we need to know the initial spectrum of spatial perturbations of the AD field when the condensate and baryon asymmetry forms at $H \approx m$. The directions ϕ_1 and ϕ_2 refer to the real and

imaginary directions as determined by the phase of the A-term. However, the phase of the A-term changes as H becomes smaller than m and $A_{\lambda o}$ comes to dominate $a_\lambda H$. Therefore,

(i) For the $|a_\lambda| \approx 1$ case, corresponding to F-term inflation, the effect is to rotate ϕ_1 and ϕ_2 such that, if we consider the relative phase of $A_{\lambda o}$ and $a_\lambda H$ to be of the order of one (corresponding to the case of a condensate with amplitude $\phi_1 \approx \phi_2$ at $H \lesssim m$), then regardless of whether $\delta\phi_1$ or $\delta\phi_2$ dominates at $H \gtrsim m$, $\delta\phi_1$ will be approximately equal to $\delta\phi_2$ once $H \lesssim m$.

(ii) If $|a_\lambda| \approx 1$ but the relative phase is much smaller than 1 (corresponding to the case of a condensate with amplitude $\phi_1 \gg \phi_2$ at $H \lesssim m$), then it is possible for $\delta\phi_2/\phi_2$ to be much larger than $\delta\phi_1/\phi_1$ at $H \lesssim m$, for example if $\delta\phi_1 \approx \delta\phi_2$ at $H \gtrsim m$ and $\phi_1 \gg \phi_2$ at $H \lesssim m$.

(iii) For the case with $a_\lambda = 0$, corresponding to D-term inflation, the initial phase of the AD field will initially be of order one relative to that of $A_{\lambda o}$, so that, as with (i), $\delta\phi_1 \approx \delta\phi_2$ and $\phi_1 \approx \phi_2$ once $H \lesssim m$.

Thus F-term inflation models can produce condensates which have different values for $\delta\phi_i/\phi_i$ ($i = 1, 2$) at $H \approx m$, whereas minimal D-term inflation models always produce roughly equal values for $\delta\phi_i/\phi_i$.

4 Linear Evolution

Because of the logarithmic correction to the AD scalar potential, there will be an attractive force between the condensate scalars which causes the spatial perturbations to grow. The inflationary perturbations are known to have a small amplitude so that the initial growth will take place in the linear regime. Condensate fragmentation and collapse to soliton lumps happens in the non-linear regime, for which the linear evolution provides calculable initial conditions. Therefore we will first consider in detail the linear evolution of the perturbations. The homogeneous AD condensate can be characterized by the charge asymmetry it carries. The condensate is generally a sum of two real oscillating scalar fields. The maximum possible charge corresponding

to a given maximum amplitude of the AD scalar occurs when the combined oscillation corresponds to a circle in the (ϕ_1, ϕ_2) plane. We will refer to this as a maximally charged (MAX) condensate. This is roughly expected to occur in the case of F-term inflation models with an order one CP violating phase and in the case of minimal D-term inflation models. The condensate can also carry a less than maximal charge, as in the case of F-term inflation models with a small CP violating phase, in which case it will describe an ellipse in the (ϕ_1, ϕ_2) plane.

4.1 MAX Condensate

A solution for the linear evolution of spatial perturbations of the condensate has been given previously for the case of a MAX condensate [7, 8], which we refer to as the Kusenko-Shaposhnikov (KS) solution [8]. It assumes a solution of the form $\phi = \phi(t) + \delta\phi(x, t)$ and $\theta = \theta(t) + \delta\theta(x, t)$, where the homogeneous MAX condensate is described by

$$\Phi = \frac{\phi(t)}{\sqrt{2}} e^{i\theta(t)} , \quad (17)$$

with $\phi(t) = (a_o/a)^{3/2} \phi_o$ (a is the scale factor) and $\dot{\theta}(t)^2 \approx m^2$, up to corrections of order Km^2 . (As it is true for most models, we will assume that $|K|$ is small compared with 1.) The KS solution also requires that $\delta\phi(x, t)$ and $\delta\theta(x, t)$ initially satisfies

$$\delta\theta_i \approx \left(\frac{\delta\phi}{\phi} \right)_i . \quad (18)$$

As discussed in the previous section, for a MAX condensate we expect $\delta\phi_1/\phi_1 \approx \delta\phi_2/\phi_2$, so that this condition is satisfied. The solution of the linear perturbation equations then has the form [7]

$$\delta\phi \approx \left(\frac{a_o}{a} \right)^{3/2} \delta\phi_o \exp \left(\int dt \left(\frac{1}{2} \frac{\mathbf{k}^2 |K| m^2}{a^2 \dot{\theta}(t)^2} \right)^{1/2} \right) e^{i\mathbf{k}\cdot\mathbf{x}} \quad (19)$$

and

$$\delta\theta \approx \delta\theta_i \exp \left(\int dt \left(\frac{1}{2} \frac{\mathbf{k}^2 |K| m^2}{a^2 \dot{\theta}(t)^2} \right)^{1/2} \right) e^{i\mathbf{k}\cdot\mathbf{x}} . \quad (20)$$

These apply if $|\mathbf{k}^2/a^2| \lesssim |2Km^2|$, H^2 is small compared with m^2 and $|K| \ll 1$. If the first condition is not satisfied, the gradient energy of the perturbations produces

a positive pressure larger than the negative pressure due to the attractive force from the logarithmic term, preventing the growth of the perturbations.

For the case of a matter dominated Universe, the exponential growth factor is

$$\int dt \left(\frac{1}{2} \frac{\mathbf{k}^2}{a^2} \frac{|K|m^2}{\dot{\theta}(t)^2} \right)^{1/2} = \frac{2}{H} \left(\frac{|K|}{2} \frac{\mathbf{k}^2}{a^2} \right)^{1/2}, \quad (21)$$

where we take the scale factor when the AD oscillations begin to be equal to 1. The largest growth factor will correspond to the largest value of \mathbf{k}^2 for which growth can occur, $\mathbf{k}^2/a^2 \approx 2|K|m^2$. Thus the value of H at which the first perturbation goes non-linear is [7]

$$H_i \approx \frac{2|K|m}{\alpha(\lambda)}, \quad (22)$$

with

$$\alpha(\lambda) = -\log \left(\frac{\delta\phi_o(\lambda)}{\phi_o} \right), \quad (23)$$

where ϕ_o is the value of ϕ when the condensate oscillations begin at $H \approx m$. A typical value of $\alpha(\lambda)$ for the spectrum Eq.(9) (e.g. for $d = 6$) is $\alpha(\lambda) \approx 30$. The initial non-linear region has a radius λ_i at H_i given by

$$\lambda_i \approx \frac{\pi}{|2K|^{1/2}m}. \quad (24)$$

Thus for a MAX condensate, when the condensate is just going non-linear, the amplitude of the scalar field is given by

$$\phi(\mathbf{x}, t) = \phi(t) + \delta\phi(\mathbf{x}, t) \approx \phi(t)(1 + \cos(\mathbf{k} \cdot \mathbf{x})), \quad (25)$$

where $|\mathbf{k}|$ is given by the wavelength which first goes non-linear, λ_i . This will provide the initial condition for the numerical study of the non-linear regime.

4.2 Non-MAX Condensate

For the case of a non-MAX condensate, we cannot directly use the KS solution. However, it is likely that the initial radius and the time at which the spatial perturbations

initially go non-linear will roughly be the same as for the MAX condensate. We will assume that $\delta\phi_1 \approx \delta\phi_2$, as is true if both scalar perturbations are maximally suppressed when $H \gtrsim m$. The equations of motion for ϕ_i ($i=1,2$) are given by

$$\ddot{\phi}_i + 3H\dot{\phi}_i - \nabla^2\phi_i = -m^2(1+K)\phi_i - Km^2\phi_i \log\left(\frac{\phi_1^2 + \phi_2^2}{\phi_o^2}\right). \quad (26)$$

For $\phi_1 \gg \phi_2$, the equation for ϕ_1 will be similar to the case of the MAX condensate, except the $\phi_1^2 + \phi_2^2$ will be oscillating in time rather than constant. Thus the equation for the growth of perturbations in ϕ_1 will be similar to the MAX condensate and the ϕ_1 perturbations will go non-linear ($\delta\phi_1/\phi_1 \gtrsim 1$) roughly as in the case of the MAX condensate. The equation for perturbation in ϕ_2 will, however, be different, since the \log term is dominated by ϕ_1^2 . The condition for the ϕ_2 equation to go non-linear is then that $\delta\phi_2 \gtrsim \phi_1$. We expect the rate of growth of $\delta\phi_2$ to be no larger than for $\delta\phi_1$, since the perturbations grow due to the attractive interaction between the scalars due to the \log term, and the interaction of ϕ_2 with $\log(\phi_1^2)$ is the same as that of ϕ_1 . So if $\delta\phi_1 \approx \delta\phi_2$ initially then we expect $\delta\phi_2 \lesssim \delta\phi_1$ throughout. Therefore non-linearity will occur only once $\delta\phi_1$ goes non-linear, at which point the condensate will begin to fragment to condensate lumps. In general, the charge density of the initial non-linear lumps will be essentially the same as that of the original homogeneous condensate.

5 Non-linear Evolution and f_B

5.1 Initial Lump

In order to study the non-linear evolution, we will consider the evolution of a single condensate lump. We can neglect the expansion of the Universe, since at the time when the spatial perturbations go non-linear, the expansion rate, H_i , is small compared with the dynamical mass scale in the equations of motion governing the growth of the lumps, $|K|^{1/2}m$, so that the $3H\dot{\phi}$ terms in the equations of motion are negligible compared with the other terms. From the discussion of Sect. 4, when the spatial perturbation is just going non-linear ($\delta\phi \approx \phi$), the AD field for the MAX condensate can be written

as

$$\Phi(x, t) \approx \frac{Ae^{imt}}{\sqrt{2}}(1 + \cos(\mathbf{k} \cdot \mathbf{x})) , \quad (27)$$

where $A/\sqrt{2}$ is the amplitude of the coherent oscillations when the field first goes non-linear. In terms of $\Phi = (\phi_1 + i\phi_2)/\sqrt{2}$, the initial non-linear perturbation is described by

$$\phi_1(\mathbf{x}, t) = A\cos(mt)(1 + \cos(\mathbf{k} \cdot \mathbf{x})) \quad (28)$$

$$\phi_2(\mathbf{x}, t) = A\sin(mt)(1 + \cos(\mathbf{k} \cdot \mathbf{x})) . \quad (29)$$

This can be thought of as a 'lattice' of adjacent condensate lumps. In order to gain some insight into the evolution of these lumps, we will consider a single spherically symmetric lump. Such lumps are described in general by

$$\phi_1(r, t) = A\cos(mt)(1 + \cos(\pi r/2r_0)) \quad (30)$$

$$\phi_2(r, t) = B\sin(mt)(1 + \cos(\pi r/2r_0)) , \quad (31)$$

for $r \leq 2r_0$ and by $\phi_{1,2} = 0$ otherwise. The initial radius of the lump is $2r_0$, where $r_0 = \pi/(\sqrt{2}|K|^{1/2}m)$. The MAX condensate lump corresponds to $A = B$, whilst the non-MAX lump has $A > B$. The corresponding energy and charge densities (with unit charge for the scalars) are

$$\rho = |\dot{\Phi}|^2 + |\nabla\Phi|^2 + V(|\Phi|) \quad (32)$$

and

$$q = \phi_1\dot{\phi}_2 - \dot{\phi}_1\phi_2 , \quad (33)$$

where

$$V(|\Phi|) = m^2|\Phi|^2 \left(1 + K \log \left(\frac{|\Phi|^2}{|\Phi|_0^2} \right) \right) . \quad (34)$$

The total energy and charge in a fixed volume are given respectively by

$$E = 4\pi \int_V dr r^2 \rho , \quad Q = 4\pi \int_V dr r^2 q \sim AB, \quad (35)$$

with, for the initial MAX condensate lump of Eqs.(30, 31),

$$Q = Q_{\max} \equiv 132.2A^2|K|^{-3/2}m^{-2} . \quad (36)$$

The non-maximally charged lump with $B < A$ then corresponds to $Q/Q_{\max} = B/A < 1$.

5.2 Numerical Solution

The scalar field equations of motion are given by Eq.(26) with $H = 0$. We have solved these equations numerically for the case of the spherically symmetric lump. We choose $A = 1$ and set $m = 100$ GeV when needed. To avoid the singularity at $|\phi| = 0$, where the one-loop logarithmic correction alone no longer is valid, we have introduced a cut-off δ by letting $(\phi_1^2 + \phi_2^2)/\phi_o^2 \rightarrow (\phi_1^2 + \phi_2^2)/\phi_o^2 + \delta$; we have verified that the value of the small cut-off does not significantly affect the solutions. With the initial lump radius $2r_0$ we have considered a spatial sphere of radius $8r_0$, at the boundary of which the outflowing waves are damped by hand. This is to prevent reflected waves bouncing back onto the lump, a situation which would be realistic only if the average lump distance were extremely small.

The behaviour of the solutions depends on K , and to a greater extent on Q/Q_{\max} . In general, the condensate lump pulsates while charge is flowing out until the lump reaches a (quasi-)equilibrium pseudo-breather configuration² (in which the lump pulsates with only a small difference between the maximum and minimum field amplitudes), as seen in Fig. 1a. We refer to this state as a Q-axiton. For non-maximal condensates, it is very different from the lowest energy configuration for a given charge, namely a Q-ball. The Q-ball is essentially made entirely of charge, with $E \approx mQ$ (neglecting the small binding energy per charge) [6, 7]. For the Q-axiton, in which the attractive force between the scalars is balanced by the gradient pressure of the scalar field, the energy per unit charge can be much larger than m ; indeed, the Q-axiton exists even if $Q = 0$. Only for a more or less maximally charged Q-axiton are the

²We distinguish between spatial pulsations of the lump as it collapses and breathing, which is essentially the coherent oscillation of the AD field within the lump.

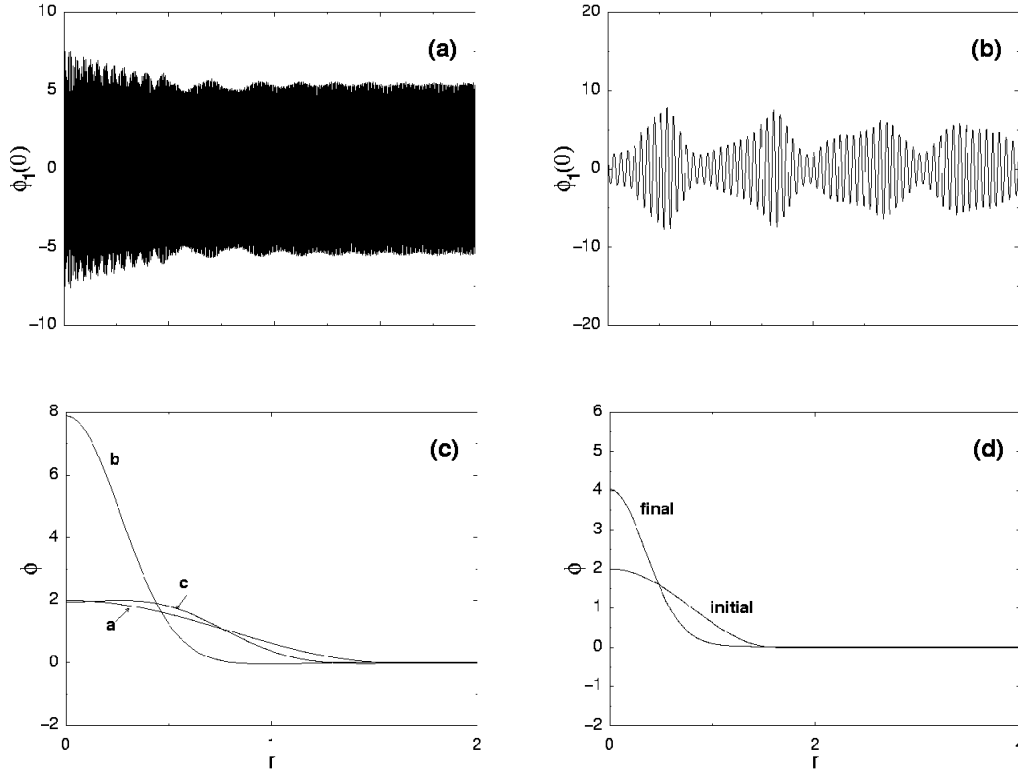


Figure 1: (a) The time evolution of the field amplitude at the origin, $\phi_1(0)$; (b) a detail of the early time evolution, showing the pulsation cycles modulating the coherent oscillations (time is in units of $1/m$); (c) the first pulsation of the condensate lump: a) initial lump; b) maximal lump; c) minimal lump; (d) the final equilibrium Q-axiton compared with the initial lump (r is in units of r_0). In all cases $K = -0.05$ and $Q = Q_{\max}$.

properties close to that of the corresponding Q-ball. We believe that the Q-axiton should eventually evolve to the lower energy Q-ball state³, although this is not apparent from our numerical results and we cannot rule out the possibility that the Q-axiton may be very long-lived. Compared with the natural time scale $t = 1/m$, the time taken to reach the Q-axiton state is long, of the order of $1600/m$ for the case $K = -0.05$ and $Q = Q_{\max}$, which is about five expansion times⁴ ($H_i^{-1} \approx 300/m$). This is shown in Fig. 1, where we display the oscillation of the field amplitude at the origin as a function of time, as well as the spatial profile of the whole lump as it pulsates. Fig.

³There are no absolutely stable spherically symmetric breather solutions in 3 + 1 flat space [14].

⁴Expansion can, however, be neglected in numerical solution for the Q-axiton itself, as noted previously.

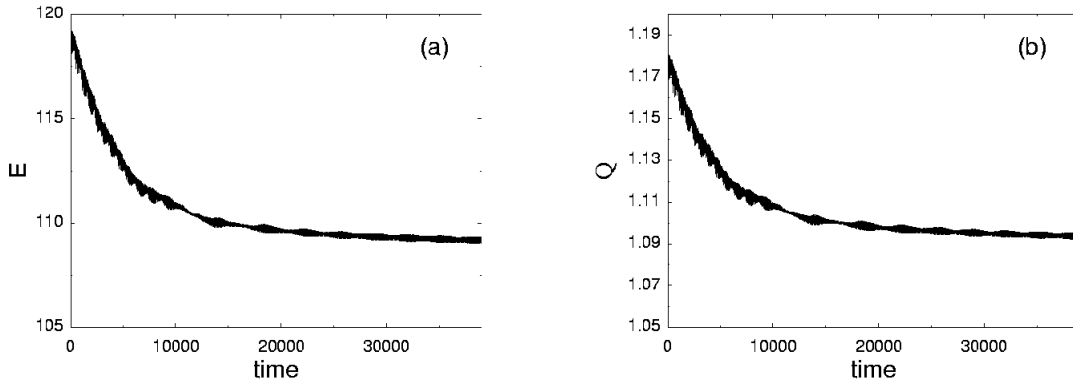


Figure 2: (a) The time evolution (in units of $1/m$) of the Q-axiton energy E and (b) charge Q for $K = -0.05$ and initial $Q = Q_{\max}$.

1a shows the rapid pulsations gradually settling towards the equilibrium by emitting scalar field waves. Fig 1b shows the first four pulsations of the lump; the high frequency oscillations modulated by the pulsations are the coherent oscillations of the AD field. The lump keeps its shape during the whole time while pulsating and slowly evolving to the final configuration, as depicted in Figs. 1c and 1d, which show the maximum amplitudes at different stages of the pulsations. In the case with $Q = Q_{\max}$, ϕ_1 and ϕ_2 have almost identical time evolution, the only difference being that there is a phase difference of $\pi/2$ between the ϕ_1 and ϕ_2 oscillations, as can easily be understood from the symmetry of the initial conditions and scalar field equations of motion.

In Fig. 2 we show the time evolution of the charge and the energy of the whole configuration, integrated out to the distance $8r_0$. At first charge and energy flows out of the volume, but the slow approach to equilibrium can also readily be seen, with the axiton lump starting with initial charge $Q = 1.18$ and stabilizing to $Q \simeq 1.09$. Q and E are nearly proportional, as they should be for the case with Q_{\max} and ϕ_1 and ϕ_2 different only by a phase $\pi/2$. (In fact, E/Q decreases from 106 GeV initially to 98 GeV, due to the increased binding energy of the Q-axiton state.) We see that for the case of the MAX condensate the ratio of E to Q is close to $m = 100$ GeV throughout, showing that the Q-axiton formed in this case is essentially a Q-ball.

In Fig. 3 we show the field amplitude and lump oscillations for the non-maximally

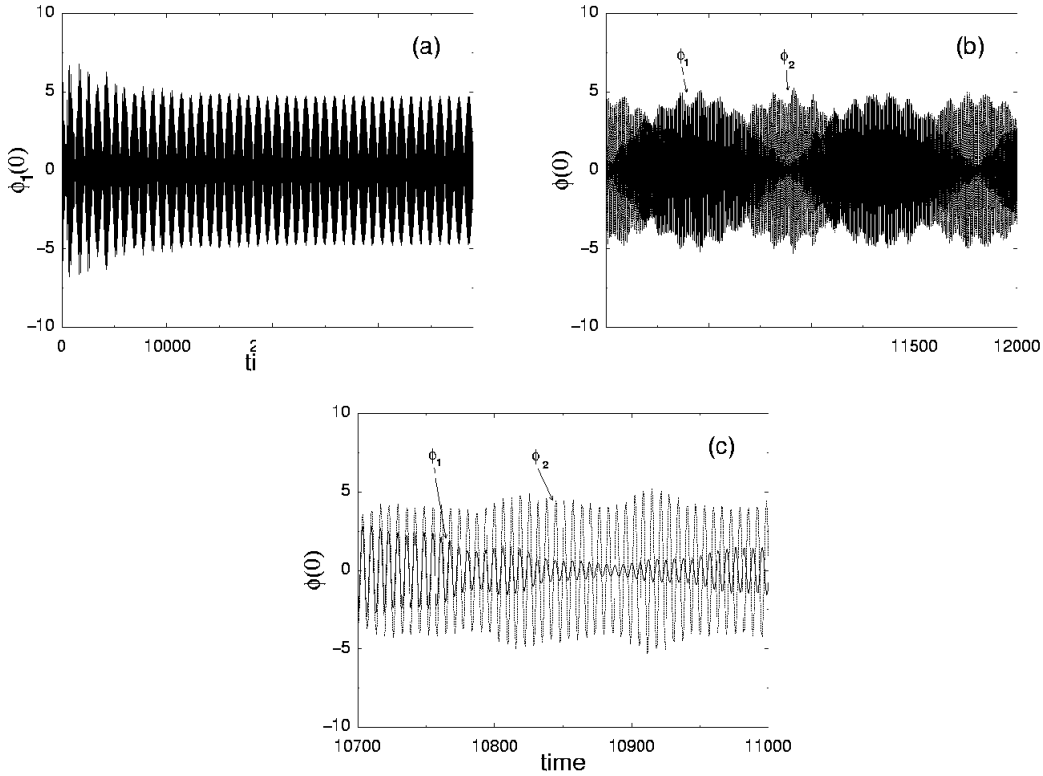


Figure 3: (a) The time evolution of the field amplitude at the origin, $\phi_1(0)$; (b) a detail of the time evolution, showing both $\phi_1(0)$ and $\phi_2(0)$; (c) a further detail. In all the cases $K = -0.05$ and $Q = 0.1Q_{\max}$ while time is in units of $1/m$

charged case $Q = 0.1Q_{\max}$. Now the squared ϕ_1 and ϕ_2 amplitudes do not follow a circle as in the maximally charged case, but rather a precessing ellipse (Fig. 3b). The qualitative behaviour is similar to the maximally charged case in that while E and Q at first escape the fiducial volume, at later times the configuration reaches a quasi-equilibrium state (Fig. 4). The initial fluctuation in Q is a numerical artifact; in general, our numerical solution for the evolution of the charge of the lump becomes less accurate for smaller Q/Q_{\max} . The ratio of E to Q of the Q-axiton in this case is approximately 600 GeV, much larger than for the corresponding Q-ball.

5.3 Values of f_B

We have also calculated f_B , the ratio of the charge in the equilibrium Q-axiton state to the charge of the initial condensate lump. The results as a function of Q and K are given in Table 1, from which we see that f_B decreases for smaller values of Q and for

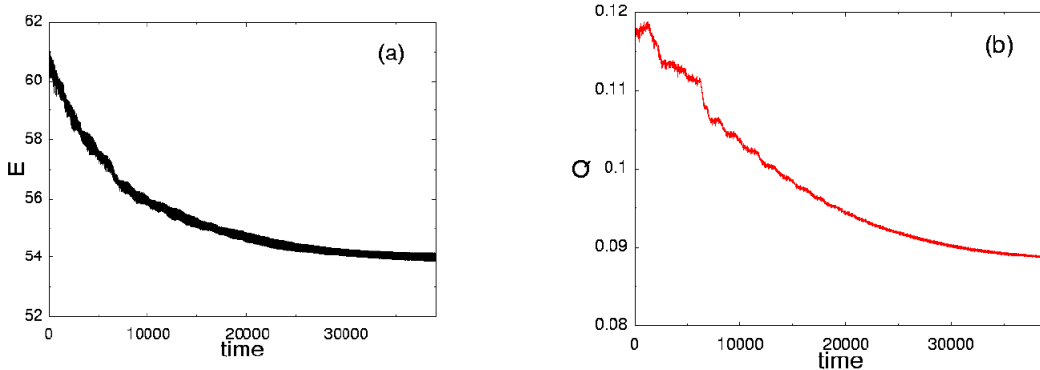


Figure 4: (a) The time evolution (in units of $1/m$) of the Q-axiton energy E and (b) charge Q for $K = -0.05$ and initial $Q = 0.1Q_{\max}$.

larger values of $|K|$.

Table 1. Values of f_B

K	Q/Q_{\max}	f_B
-0.1	1	0.89
-0.05	1	0.92
-0.01	1	0.94
-0.1	0.1	0.64
-0.05	0.1	0.74
-0.01	0.1	0.83
-0.1	0.01	~ 0.3
-0.05	0.01	~ 0.5
-0.01	0.01	~ 0.6

In all this we have considered a single spherically symmetric lump isolated in space, compared with the real case in which there is a lattice of closely spaced lumps which are in general not spherically symmetric. It is beyond the scope of the present paper to study this more realistic case, but we note that the rate at which the lumps radiate charge and energy is very slow. By the time the lumps have radiated their charge and reached the Q-axiton state, they will have been substantially pulled apart by

expansion, so that the lumps are eventually isolated. Therefore the results for f_B for the spherically symmetric lump are likely to be a reasonable estimate of the values in the realistic case. Indeed, since we might expect non-spherically symmetric lumps to be less efficient in reaching their quasi-equilibrium configurations, the values of f_B for the spherically symmetric lump may well be an underestimate of the realistic value. We will assume in the following that the Q-axitons eventually evolve to lower energy Q-balls of the same charge. To do this they must lose their excess energy, presumably by a very slow radiation of scalar field waves. However, the full evolution of the Q-axiton to the final Q-ball requires a much more ambitious numerical analysis than that attempted here.

6 Consequences for Affleck-Dine Baryogenesis

We have previously discussed the possibility that Q-balls can decay at a very low temperature, $T_d \lesssim 1$ GeV. Such low decay temperatures naturally occur for the case of $d = 6$ AD baryogenesis, which has a reheating temperature typically around 1 GeV [7, 16]. Late decaying Q-balls (“B-ball baryogenesis” [6, 7]) can both protect the baryon asymmetry from the effects of L violating interactions (such as arise with Majorana neutrino masses) and allow for an understanding of why the number density of baryons and dark matter particles are within an order of magnitude of each other when the dark matter particles have masses of the order of m_W . In the case where the similarity of the number densities is explained by the late decay of Q-balls to lightest SUSY particles (LSPs) and baryons, the value of f_B immediately gives us the mass of the LSP. The ratio of the number densities is given by [5, 7]

$$\frac{n_B}{n_{DM}} = \frac{1}{3f_B} \quad (37)$$

The observed range of ratios is [16]

$$\left(\frac{n_B}{n_{DM}} \right)_{obs} = (1.5 - 7.3) \frac{m_{LSP}}{m_W} . \quad (38)$$

To be consistent with present experimental limits on MSSM neutralinos, $m_\chi \gtrsim 30$ GeV [20], we would require that $f_B \lesssim 0.6$. From Table 1 we see that this rules out MSSM

neutralinos as the LSP for K in the range -0.1 to -0.01 and $Q/Q_{max} \geq 0.1$. However, for $Q/Q_{max} = 0.01$ it is probable that, for sufficiently large $|K|$, light MSSM neutralinos from Q-ball decay can be consistent with experimental bounds. Our numerical results become less accurate for smaller values of Q and larger $|K|$, but we expect that MSSM neutralinos up to 60 GeV can be consistent with experimental limits for $K = -0.1$ and $Q/Q_{max} = 0.01$. It is interesting to note that a recent dark matter search experiment has suggested the existence of a candidate of mass 59 GeV [21]. It should be kept in mind that in the realistic non-spherically symmetric case f_B could well be smaller, so allowing for larger neutralino masses. On the other hand, if $f_B \gtrsim 0.6$, then either we must allow the neutralinos to annihilate after Q-ball decay, so breaking the direct connection between the number densities of baryons and dark matter particles [5, 7], or we must go beyond the MSSM. A light singlino in the next-to-minimal SUSY Standard Model (NMSSM) would be an interesting possibility for the LSP in this case [22].

This all assumes that the Q-axitons evolve into the corresponding Q-balls. Should the Q-axitons be very long-lived, their cosmology, for the case of a non-MAX condensate, could be substantially different from that of the Q-balls .

7 Conclusions

We have considered the origin and linear evolution, in the context of SUSY F- and D-term inflation models, of spatial perturbations of an Affleck-Dine condensate and the collapse of a spherically symmetric condensate lump of the type expected to arise from the fragmentation of the condensate. We find that for a typical range of parameters, 30-90 % of the charge of the collapsing lump ends up in the final quasi-equilibrium state ($f_B \approx 0.3 - 0.9$), with the remainder being radiated in the form of ripples of scalar field. The quasi-equilibrium state is, in general, not a Q-ball, but a higher energy pseudo-breather state, a Q-axiton. This physically approximates a Q-ball only for the case of an initial condensate which is nearly maximally charged. Assuming that the Q-axiton evolves into the corresponding Q-ball, for the case where dark matter and

baryons originate directly from late-decaying Q-balls, so explaining the similarity of the number densities of baryons and dark matter particles, $f_B \lesssim 0.6$ allows for a range of neutralino masses consistent with experimental constraints on MSSM neutralinos. Such values can occur if the condensate is not maximally charged. $f_B \gtrsim 0.6$, on the other hand, requires $m_{LSP} \lesssim 30$ GeV, which rules out MSSM neutralinos coming directly from late-decaying Q-balls as dark matter, although an NMSSM singlino could be consistent with experimental constraints. The numerical results presented here are based on the evolution of a single, isolated, spherically symmetric condensate lump. To study Affleck-Dine condensate collapse for the realistic case, with many condensate lumps of different shapes and sizes, and to study the evolution of the Q-axitons into Q-balls, we would require a much more ambitious numerical analysis than that presented here. We hope to develop this in the future.

Acknowledgements

This work has been supported by the Academy of Finland and by the UK PPARC.

References

- [1] I.A.Affleck and M.Dine, *Nucl. Phys.* **B249** (1985) 361.
- [2] A.Riotto and M.Trodden, *hep-ph/9901362*.
- [3] H.P.Nilles, *Phys. Rep.* **110** (1984) 1.
- [4] K.Enqvist and J.McDonald, *hep-ph/9811412* (*To be published in Phys.Rev.Lett.*).
- [5] K.Enqvist and J.McDonald, *Phys. Lett.* **B440** (1998) 59.
- [6] K.Enqvist and J.McDonald, *Phys. Lett.* **B425** (1998) 309.
- [7] K.Enqvist and J.McDonald, *Nucl. Phys.* **B538** (1999) 321.
- [8] A.Kusenko and M.Shaposhnikov, *Phys. Lett.* **B418** (1998) 46.
- [9] A.Kusenko, *Phys. Lett.* **405** (1997) 108.

- [10] G.Dvali, A.Kusenko and M.Shaposhnikov, *Phys. Lett.* **B417** (1998) 99.
- [11] M.Dine, W.Fischler and D.Nemeschansky, *Phys. Lett.* **B136** (1984) 169; G.D.Coughlan, R.Holman, P.Ramond and G.G.Ross, *Phys. Lett.* **B140** (1984) 44; E.Copeland, A.Liddle, D.Lyth, E.Stewart and D.Wands, *Phys. Rev.* **D49** (1994) 6410; E.D.Stewart, *Phys. Rev.* **D51** (1995) 6847; M.Dine, L.Randall and S.Thomas, *Phys. Rev. Lett.* **75** (1995) 398; G.Dvali, *hep-ph/9503259*.
- [12] M.Dine, L.Randall and S.Thomas, *Nucl. Phys.* **B458** (1996) 291.
- [13] S.Coleman, *Nucl. Phys.* **B262** (1985) 263.
- [14] E.Kolb and I.Tkachev, *Phys. Rev.* **D49** (1994) 5040.
- [15] J.Hormuzdiar and S.Hsu, *hep-th/9906058*.
- [16] J.McDonald, *hep-ph/9901453*.
- [17] C.Kolda and J.March-Russell, *hep-ph/9802358*.
- [18] J.Ellis, J.E.Kim and D.V.Nanopoulos, *Phys. Lett.* **145B** (1984) 181; S.Sarkar, *Rep. Prog. Phys.* **59** (1996) 1493.
- [19] E.W. Kolb and M.S. Turner, *The Early Universe* (Addison-Wesley, Reading MA, USA, 1990).
- [20] C. Caso *et al.* (Particle Data Group), *Eur. Phys. J.* **C3** (1998) 1.
- [21] A.Bottino, F.Donato, N.Fornengo and S.Scopel, *Phys. Lett.* **B423** (1998) 109.
- [22] U.Ellwanger, M.Raush de Traubenberg and C.A.Savoy, *Nucl. Phys.* **B492** (1997) 21.